scientific **data**

Check for updates

DATA DESCRIPTOR

A comprehensive dataset of photonic features on spectral converters for energy harvesting

Rute A. S. Ferreira[1] ✉, Sandra F. H. Correia[2], Petia Georgieva[2,3], Lianshe Fu[1], Mário Antunes[2,4] & Paulo S. André[5] ✉

Building integrated photovoltaics is a promising strategy for solar technology, in which luminescent solar concentrators (LSCs) stand out. Challenges include the development of materials for sunlight harvesting and conversion, which is an iterative optimization process with several steps: synthesis, processing, and structural and optical characterizations before considering the energy generation figures of merit that requires a prototype fabrication. Thus, simulation models provide a valuable, cost-effective, and time-efficient alternative to experimental implementations, enabling researchers to gain valuable insights for informed decisions. We conducted a literature review on LSCs over the past 47 years from the Web of Science™ Core Collection, including published research conducted by our research group, to gather the optical features and identify the material classes that contribute to the performance. The dataset can be further expanded systematically offering a valuable resource for decision-making tools for device design without extensive experimental measurements.

Background & Summary

The luminescent solar concentrator (LSC) concept (Fig. 1a) dates from the late 70 s[1,2], but major advances occurred over the last twenty years. Nowadays, LSCs are seen as an urban architecture strategy to integrate solar-harvesting devices into buildings, Fig. 1a,b[3]. This was greatly fostered by the introduction of the Zero-Energy Building (ZEB) concept and related United Nations and European Union directives[4–6]. The implementation of ZEBs implies an optimized use of renewable energy sources which draws attention to solutions that may easily contribute to the energy efficiency of buildings, through existing infrastructures and, thus, LSCs gained renewed importance over the last decade, with real-life demonstrators being developed and implemented (e.g. highway sound barriers[7–10] and agrivoltaic applications[11,12]) and companies being founded (e.g. *Glass to Power*[13], *UbiQD*[14] and *ClearVue*[PV])[15]. A step further on LSC development was the recently reported approach including additional sensing abilities to LSCs to behave as sunlight-powered optical temperature sensors[16,17], which would make possible the optimization of heating/cooling systems without the need for additional energy-consuming sensors or systems, enabling substantial long-term benefits for society concerning energy consumption habits. Moreover, material science has evolved hugely over the last years in terms of achieving optically active materials with high absorption and conversion ability and small overlap between the absorption and emission spectra to prevent re-absorption losses (e.g. large Stokes-shift[18,19] defined for organic molecules), which enabled the fabrication of large-area devices[18,20–29]. An LSC consists of planar waveguides that are either doped or coated with emissive materials. These materials absorb sunlight and re-emit it at distinct wavelengths that match the operating spectral region of the photovoltaic (PV) cells. The emitted light is then guided through total internal reflection towards photovoltaic cells coupled to the edges of the waveguides, where it is converted into electricity.

[1]Department of Physics and CICECO—Aveiro Institute of Materials, University of Aveiro, 3810-193, Aveiro, Portugal. [2]Instituto de Telecomunicações, University of Aveiro, 3810-193, Aveiro, Portugal. [3]Departament of Electronics, Telecommunications and Informatics, Institute of Electronics and Informatics Engineering of Aveiro (IEETA), University of Aveiro, 3810-193, Aveiro, Portugal. [4]Department of Electronics, Telecommunications and Informatics, University of Aveiro, 3810-193, Aveiro, Portugal. [5]Department of Electrical and Computer Engineering and Instituto de Telecomunicações, Instituto Superior Técnico, Universidade de Lisboa, 1049-001, Lisbon, Portugal. ✉e-mail: rferreira@ua.pt; paulo.andre@lx.it.pt
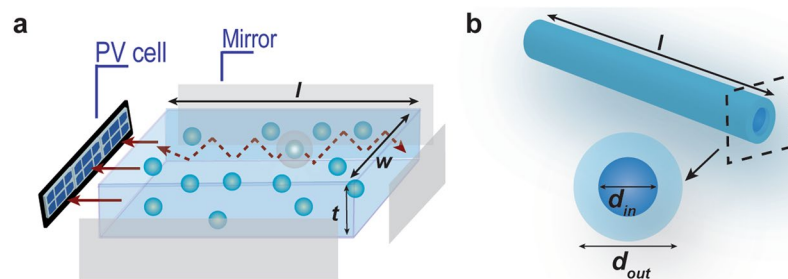
Fig. 1 Luminescent solar concentrator concept. Scheme of (**a**) planar and (**b**) fiber-based LSC with dimensions: (*l* – length, *w* – width, *t* – thickness, d_{in} – inner diameter, d_{out} – outer diameter) in the hollow-core configuration. In this case, the doped layer is in the core (d_{in}). The 4 edges of the planar LSCs may be coupled to PV cells or mirrors (or reflective tapes).

The optical conversion efficiency (η_{opt}) is widely recognized as the primary figure of merit to evaluate the performance of LSCs. It quantifies the ratio of the generated output optical power (P_{out}) to the incident optical power (P_{in}), providing a measure of how effectively the materials convert incoming light into usable optical signal[19]. This figure of merit serves as a crucial benchmark for evaluating the efficacy of various approaches and optimizing LSC configurations to enhance overall efficiency.

Another parameter commonly used to quantify performance in terms of light harvesting and energy conversion is the power conversion efficiency (PCE). The PCE measures the ratio of the generated electrical power (P_{out}^{el}) to P_{in}, taking into account the specific characteristics of the coupled photovoltaic cell. The PCE provides a more comprehensive assessment of the LSC's performance by considering the electrical power and the photovoltaic cell's efficiency.

Despite enormous efforts, the improvement in these figures of merit is somewhat limited. Unless the intrinsic limitations, such as low absorption efficiency coefficient translated into weak radiation-harvesting capability, large self-absorption quantified by the spectral overlap between the emission and the absorption spectrum, and poor conversion efficiency quantified by a low emission quantum yield η_{yield} can be solved, it seems unrealistic to use these materials for solar energy conversion and to be active in climate change-related actions and substantial long-term benefits for society. In addition, self-absorption quantified by the overlap integral OI[30] between the absorption and emission spectra (in some cases presented as the modified overlap integral $OI*$[31,32] if normalized to the emission spectra) has been pointed out as one of the most critical aspects for the device performance[3,19,30–34], although its quantification is available in very few works[30–32]. Nevertheless, bearing in mind the final goal of large-scale implementation in real applications, transparency and visible light transmittance are also key factors when thinking of replacing windows with such devices. Thus, a balance between the visual comfort of the building occupants and electrical output should be achieved.

In 1988, John Maddox wrote, "One of the continuing scandals of physical science is that it remains, in general, impossible to predict the structure of even the simplest crystalline solids from a knowledge of their chemical composition"[35]. While facing some evolution nowadays, predicting the crystal structure based solely on the composition remains challenging and entails high computational costs. An even more glaring example is the *a priori* prediction of materials compositions from the massive amount of produced and published experimental data, for a given set of target applications, as the rationalization of materials is exceptionally difficult.

Although several reviews on LSCs have been published over the years[3,19,33,36–47], mostly concerning the type of luminescent materials in use and LSC configurations and applications, this dataset intends to go further and be a starting point to achieve a massive compilation of relevant features concerning optically active materials used to fabricate LSCs, which can be helpful for researchers working in the field. Also, this dataset has the potential to promote much-needed standardization in the reporting of figures of merit and characterization procedures for LSC devices, which is a concern[48,49]. By establishing consistent reporting practices, researchers and industry professionals can ensure comparability, reproducibility, and effective collaboration in the field.

Methods

The dataset was collated from the community of researchers or research groups working in the development of LSC and all data sources are cited[1,11,16–18,20–30,32,50–231]. The first paper reporting the concept of LSC dates from 1976[1,2], setting the starting point for the literature review behind the dataset. This literature review starting over the past 47 years on the field of spectral energy conversion was made using CitNetExplorer and VOSViewer tools. The sample data consisting of the information from 1474 published articles, letters, reviews, and books from the Web of Science™ Core Collection containing the following citation indexes: SCI-EXPANDED, SSCI, A&HCI, CPCI-S, CPCI-SSH, ESCI, CCR-EXPANDED, and IC, using the search terms in all fields: luminescent solar concentrator or fluorescent collector or greenhouse collector in the period from 1976 to 2023, accessed on November 16, 2023. This approach has been successfully used in the field of optical sensing[232,233]. From each article, information was extracted such as authors' names, affiliation and funding entity, the document title, keywords, abstract, and reference list, the publication citations and date, and the journal information, allowing for analyzing these fields in a multitude of parameters. We explored these fields by creating a map based on text categorical data (Fig. 2), which means that the abstracts, keywords, and titles were scanned for terms or verified whether a term is present or not (binary counting) and if it has a link with some other terms
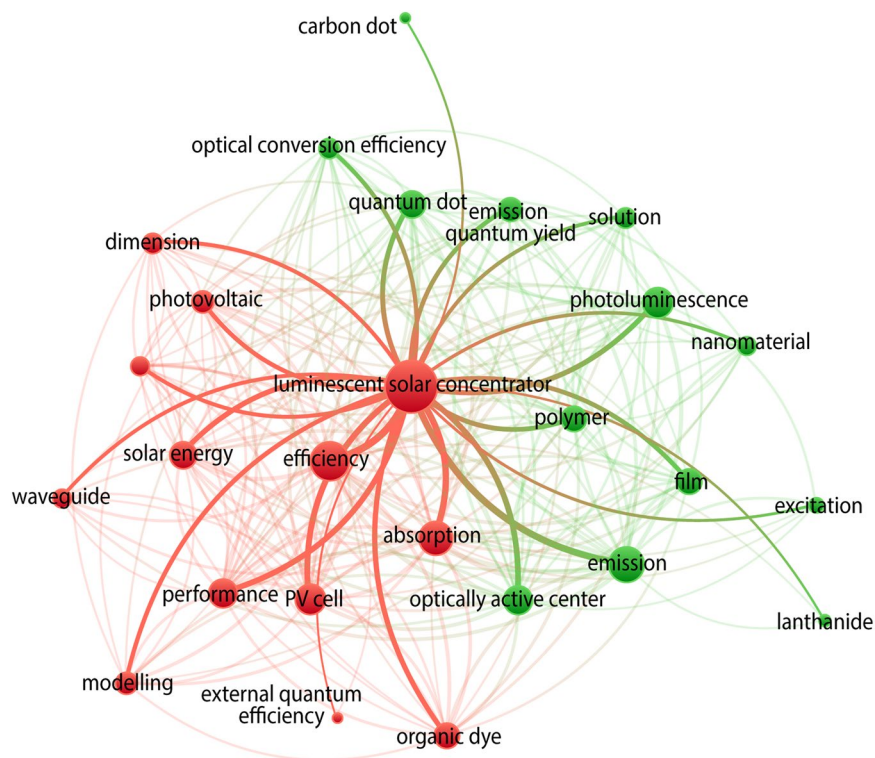
Fig. 2 Network visualization of term occurrences extracted from abstracts and titles in 1322 publications from Web of Science™ principal collection in the period 1976–2023, using 'luminescent solar concentrator' as the search keyword. A threshold cutoff of 10 as a number of term co-occurrence was used. The diameter of the circles is directly proportional to the number of occurrences of an indexing term, and the distance is directly proportional to the relation between them on the map (the closer two indexing terms are the more related they are). The highlighted lines represent the direct connections with the 'luminescent solar concentrator' term.

(both appearing in the same document). If the term appeared in a document, it is counted as one occurrence and if two terms appear together in the same document (co-occurrence), a link is created between them. The number of occurrences of a term was represented by the relative size of its circle. The categories, features and terms included in the dataset were chosen considering the more recurrent terms which is directly related to their relevance in the field. Also, the proximity of terms in the map was representative of how closely related they were, despite having a co-occurrence or not. Nevertheless, in some cases, a term linked with many other terms that were not related, can appear at a longer distance, being placed in the middle of all its connections. There was also the aggregation of terms that were homonyms but had different designations amongst the published papers. Based on these connections and the terms found in the research, it is possible to define two main clusters containing terms that are representative of different fields of study: one related to LSC devices and the other one related to photoluminescence spectroscopy (Fig. 2). The most relevant terms which are directly connected with the 'luminescent solar concentrator' term are highlighted in Fig. 2 and those are the ones addressed in the dataset here reported. The optical features and the materials classes are the links between the clusters as the indexing terms such as, for instance, emission, absorption, quantum yield, lanthanide, carbon dot, dimension, or film are shared[234,235].

The dataset is composed of a description of the materials used to fabricate the LSC device, in what concerns the optically active centres type and concentration, the host material, and the processing methods. Only downshifting examples were considered as they are the vast majority of reported cases, although LSCs based on other energy conversion mechanisms such as upconversion[236,237] or downconversion[238] are already available. Numerical data (when available) were also manually extracted from each of the published papers to compose the table dataset. The numerical values considered for the optical characterization parameters include: i) wavelength of peak absorption or excitation (A_p), ii) minimum wavelength of the absorption or excitation spectral band (A_{min}), iii) maximum wavelength of the absorption or excitation spectral band (A_{max}), iv) wavelength of peak emission (E_p), v) minimum wavelength of the emission spectral band (E_{min}), vi) maximum wavelength of the emission spectral range (E_{max}), and vii) emission quantum yield (η_{yield})[239]. The general optical features are based on photoluminescence data and absorption spectra. Figure 3 illustrates the excitation and emission spectra of one reported LSC based on lanthanide ions[110] in which the relevant parameters were assigned as follows:

(i) A_p: wavelength at which the intensity reaches a peak value in the excitation (or absorption) spectrum measured in nanometres (nm).

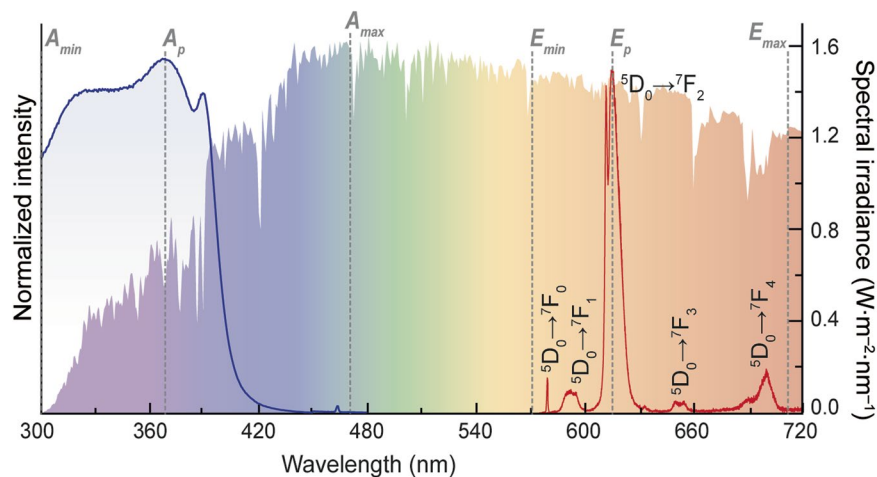(ii) E_p: wavelength at which the emission spectrum has a maximum intensity value, measured in nm.

Fig. 3 Optical features description. Excitation spectrum monitored at 612 nm and emission spectrum excited at 370 nm for a selected Eu^{3+}-based organic-inorganic hybrid[110]. The shadowed area represents the Air Mass 1.5 Global solar spectrum (AM1.5 G, the spectrum generally used in terrestrial solar cell research, right y axis).

(iii) A_{min}: low-wavelength value of the excitation (or absorption) spectrum, measured in nm. In most cases, the value of 300 nm is considered as a threshold because below this the solar irradiance is very low ($\sim10^{-4}$% of the total solar irradiance on Earth).

(iv) A_{max}: high-wavelength value of the excitation (or absorption) spectrum, where the intensity exhibits significant deviation from the noise level ($>$5%), measured in nm.

(v) E_{min}: low-wavelength value of the emission spectrum, where the intensity exhibits significant deviation from the noise level ($>$5%), measured in nm.

(vi) E_{max}: high-wavelength value of the emission spectrum, where the intensity exhibits significant deviation from the noise level ($>$5%), measured in nm.

Hence, the compiled dataset is highly representative of the field, capturing a comprehensive range of optical properties and characteristics about LSCs and related materials.

The dataset is also composed of the so-called performance features like η_{opt} and PCE, which are intrinsically dependent on the dimensions of the LSC device (Fig. 1a,b), and thus this information is also provided in the dataset. By definition, η_{opt} is a measure of the ratio between the output optical power and the incident one:

$$\eta_{opt} = \frac{P_{out}}{P_{in}}$$

(1)

Experimental optical measures of P_{out} and P_{in} are performed using integrating spheres or power meters to calculate η_{opt} using Eq. 1 (from this point onwards, it will be referred to as the definition equation). These parameters can also be estimated when the LSCs are coupled to a photovoltaic cell. In this scenario, the literature provides various models (expressions) that can be employed to establish a correlation between the measured electrical parameter in the photovoltaic cell and the optical power. These models offer different levels of accuracy, allowing for a more comprehensive analysis of the relationship between the two variables. Among these, Eqs. 2, 3 are frequently employed to quantify η_{opt}. While Eq. 2 (higher accuracy equation) provides high accuracy by precisely incorporating the efficiency of the PV cell to correct the spectral response, Eq. 3 (lower accuracy equation) is a rougher approximation. Equation 2 is defined as follows[50]:

$$\eta_{opt} = \frac{I_{SC}^L V_0^L}{I_{SC} V_0} \frac{A_e}{A_s} \frac{\eta_{solar}}{\eta_{PV}}$$

(2)

where I_{SC}^L and V_0^L represent the short-circuit current and the open voltage of the photovoltaic cell coupled to the LSC, respectively (I_{sc} and V_0 are the corresponding values of the photovoltaic cell exposed directly to solar radiation), η_{solar} is the efficiency of the photovoltaic cell relative to the total solar spectrum, η_{PV} is the efficiency of the photovoltaic cell at the LSC emission wavelengths, A_e is the LSC edge area, and A_s is the top surface area of the LSC[50]. An alternative definition, Eq. 3, is given by[170]:

$$\eta_{opt} = \frac{I_{SC}^L}{I_{SC}} \frac{A_e}{A_s}$$

(3)

There is also more theoretical approach (theoretical equation), which considers that η_{opt} can be described by weighting all the main optical losses found in the LSC (most of them can be assessed experimentally), given by the product of the several terms in Eq. 4[240]:

$$\eta_{opt} = (1 - R)\eta_{abs}\eta_{SA}\eta_{yield}\eta_{Stokes}\eta_{trap}\eta_{mat} \tag{4}$$

in which R is the Fresnel reflection coefficient for perpendicular incidence, η_{abs} is the ratio of photons absorbed by the emitting layer to the number of photons falling on it, η_{SA} is the self-absorption efficiency[241], η_{Stokes} is the Stokes efficiency, η_{trap} is the trapping efficiency and η_{mat} takes into account the transport losses due to matrix absorption and scattering. This suggests that different equations yield comparable results in terms of optical conversion efficiency. However, it is worth noting that Eq. 3 is more commonly utilized.

The PCE figure of merit is obtained from experimental data using the following Eq. 5:

$$PCE = \frac{P_{out}^{el}}{P_{in}} = \frac{I_{SC}^L V_{oc}^L FF}{A_S \int_{\lambda_1}^{\lambda_2} I_{AM1.5G}(\lambda)\,d\lambda} \tag{5}$$

where FF is the fill factor of the photovoltaic cell. The PCE figure of merit correlates the output electrical power (which is directly dependent of the PV cell in use) to the incident optical one.

We note that the number of entries in the dataset is somewhat limited because, although the number of publications is increasing over the last 15 years (total publications ∼1500), there is a significant amount (∼80%) of published works on luminescent solar concentrators which lack performance quantification related either to η_{opt} or to PCE. This results in ∼300 published works with LSC performance quantification, matching the number of entries in the dataset.

Data Records
The complete dataset is available at *figshare*[242]. The data is contained in an Excel file (.xlsx file, composed of 27 columns and 305 entries, which provides the data and the details of the dataset. The here presented dataset has the key to columns and units presented in the following tables, divided in two types: i) materials and the manufacturing processing categories (Table 1) and ii) numerical values considered for the optical features and electrical characterization parameters (Table 2). Table 3 describes the columns which were included in the dataset to facilitate identification and tracking of the reported LSC, such as designation, publication year and DOI of the source published work.

Technical Validation
To ensure data integrity and quality, only data extracted from published works in SCI-indexed journals were considered. The data related with spectroscopic features (emission and absorption/excitation) were either taken directly from the text when the figures were fully described or extracted from presented graphs (spectra), which may cause some value misreading, inducing an estimated deviation of ±10 nm. For numerical data (*OI*, *OI**, η_{yield}, η_{opt} and PCE), the values were extracted from the main text as reported by the authors. In what concerns the experimental data, the spectroscopic data presents the deviation associated with the measuring equipment, which is typically around 2 nm. For the η_{yield}, it is important to note that the values are typically within a 10% error range, as typically stated by the manufacturer of the integrating spheres apparatus, probably related with detector sensitivity limitations and software calculations.

The error associated with the calculated values of η_{opt} and PCE was estimated using the error propagation method, which generally induces a relative error of $\Delta\eta_{opt}/\eta_{opt}$ and $\Delta PCE/PCE$ below 5%. The η_{opt} associated error is given by:

$$
\begin{aligned}
(\Delta\eta_{opt})^2 &= \left(\frac{d\eta_{opt}}{dI_{sc}^L}\Delta I_{sc}^L\right)^2 + \left(\frac{d\eta_{opt}}{dV_0^L}\Delta V_0^L\right)^2 + \left(\frac{d\eta_{opt}}{dA_e}\Delta A_e\right)^2 + \left(\frac{d\eta_{opt}}{d\eta_{solar}}\Delta h_{solar}\right)^2 \\
&\quad + \left(\frac{d\eta_{opt}}{dI_{sc}}\Delta I_{sc}\right)^2\left(\frac{d\eta_{opt}}{dV_0}\Delta V_0\right)^2 + \left(\frac{d\eta_{opt}}{dA_s}\Delta A_s\right)^2 + \left(\frac{d\eta_{opt}}{d\eta_{PV}}\Delta\eta_{PV}\right)^2 \\
&= \left(\frac{V_0^L A_e \eta_{solar}}{I_{sc}V_0 A_s \eta_{PV}}\Delta I_{sc}^L\right)^2 + \left(\frac{I_{sc}^L A_e \eta_{solar}}{I_{sc}V_0 A_s \eta_{PV}}\Delta V_0^L\right)^2 + \left(\frac{I_{sc}^L V_0^L \eta_{solar}}{I_{sc}V_0 A_s \eta_{PV}}\Delta A_e\right)^2 \\
&\quad + \left(\frac{I_{sc}^L V_0^L A_e}{I_{sc}V_0 A_s \eta_{PV}}\Delta\eta_{solar}\right)^2 + \left(-\frac{I_{sc}^L V_0^L A_e \eta_{solar}}{(I_{sc})^2 V_0 A_s \eta_{PV}}\Delta I_{sc}\right)^2 \\
&\quad + \left(-\frac{I_{sc}^L V_0^L A_e \eta_{solar}}{I_{sc}(V_0)^2 A_s \eta_{PV}}\Delta V_0\right)^2 + \left(-\frac{I_{sc}^L V_0^L A_e \eta_{solar}}{I_{sc}V_0 (A_s)^2 \eta_{PV}}\Delta A_s\right)^2 \\
&\quad + \left(-\frac{I_{sc}^L V_0^L A_e \eta_{solar}}{I_{sc}V_0 A_s (\eta_{PV})^2}\Delta\eta_{PV}\right)^2
\end{aligned}
\tag{6}
$$

where $\Delta I_{sc}^L = \Delta I_{sc} = 10^{-10}A$ and $\Delta V_0^L = \Delta V_0 = 10^{-3}V$ (assuming an usual multimeter, as the 2400 SourceMeter SMU Instruments, Keithley), $\Delta\eta_{solar} = \Delta_{PV} = 0.01$ and ΔA_e and ΔA_s account for the error in

Header	Explanation	Unit	Classes
type_OC	the optically active centre type	—	• dye - organic dye • Ln - lanthanide ions • QD - quantum dot • CD - carbon dot • NP - nanoparticle • polymer • a combination of the above
chemical_OC	the chemical designation of the optically active centre	—	—
concentration	the optically active centre concentration	• M • wt%	—
type_h	the material host	—	• hybrid • polymer • solvent • resin • glass
chemical_h	the chemical designation of the host material	—	—
processing	the host material processing method	—	• film • bulk • solution • fiber
method	the LSC fabrication method	—	• drop cast • spin-coating • dip-coating • spray-coating • doctor blade • liquid in container • 3D printing • scrap-coating
conditions_η_{opt}	experimental measurement conditions used in the determination of the optical conversion efficiency η_{opt}	—	—
conditions_PCE	experimental measurement conditions used in the determination of the power conversion efficiency PCE	—	—
PV cell	photovoltaic cell used in the LSC performance quantification	—	• a-Si - amorphous Silicon • c-Si - crystalline Silicon • GaAs • Perovskite • CIGS - Copper Indium Gallium Selenide • Organic • CuInSe$_2$ • DSSC – dye-sensitized solar cell

Table 1. Parameters included in the dataset related to the materials and the manufacturing processing.

Header	Explanation	Unit
dimension	LSC dimension: l × w × t for bulk/film or l × d_{out} × d_{in} (when applicable) for fibers. See Fig. 1a,b for clarification.	cm
A_p	wavelength value for the peak absorption	nm
A_{min}	minimum wavelength value for the absorption spectral band	nm
A_{max}	maximum wavelength value for the absorption spectral band	nm
E_p	wavelength value for the peak emission	nm
E_{min}	minimum wavelength value for the emission spectral band	nm
E_{max}	maximum wavelength value for the emission spectral band	nm
OI	overlap integral between absorption and emission bands	[a]
OI*	overlap integral between absorption and emission bands normalized to the emission one	[a]
η_{yield}	emission quantum yield	%
η_{opt}	optical conversion efficiency	%
PCE	power conversion efficiency	%

Table 2. Parameters included in the dataset related to numerical values considered for the optical and electrical performance quantification. [a]Absolute values.

Header	Explanation
designation	designation used to describe the LSC: optical centre – host
year	the publication year of the source paper from which the data is obtained
DOI	the source paper DOI, allowing for easy identification and citation

Table 3. Other information provided in the dataset related to the listed devices.

measuring the LSC dimensions, which can be done using a measuring tape/ruler or a caliper with a 5×10^{-4} or 5×10^{-5} m error, respectively.

The *PCE* associated error is given by:

$$
\begin{aligned}
(\Delta PCE)^2 &= \left(\frac{dPCE}{dI_{sc}^L}\Delta I_{sc}^L\right)^2 + \left(\frac{dPCE}{dV_0^L}\Delta V_0^L\right)^2 \\
&\quad + \left(\frac{dPCE}{d\int_{\lambda_1}^{\lambda_2} I_{AM1.5G}(\lambda)d\lambda}\Delta\int_{\lambda_1}^{\lambda_2} I_{AM1.5G}(\lambda)d\lambda\right)^2 + \left(\frac{dPCE}{dA_S}\Delta A_s\right)^2 \\
&= \left(\frac{V_0^L FF}{A_S \int_{\lambda_1}^{\lambda_2} I_{AM1.5G}(\lambda)d\lambda}\Delta I_{sc}^L\right)^2 + \left(\frac{I_{sc}^L FF}{A_S \int_{\lambda_1}^{\lambda_2} I_{AM1.5G}(\lambda)d\lambda}\Delta V_0^L\right)^2 \\
&\quad + \left(\frac{I_{sc}^L V_0^L FF}{A_S \left(\int_{\lambda_1}^{\lambda_2} I_{AM1.5G}(\lambda)d\lambda\right)^2}\Delta\int_{\lambda_1}^{\lambda_2} I_{AM1.5G}(\lambda)d\lambda\right)^2 \\
&\quad + \left(\frac{I_{sc}^L V_0^L FF}{(A_S)^2 \int_{\lambda_1}^{\lambda_2} I_{AM1.5G}(\lambda)d\lambda}\Delta A_S\right)^2
\end{aligned}
\tag{7}
$$

where $\Delta\int_{\lambda_1}^{\lambda_2} I_{AM1.5G}(\lambda)d\lambda = 0.01\ W \cdot m^{-2}$.

Usage Notes

The dataset presented in this work intends to be a pivotal resource for researchers and engineers working on the field of optical materials for down-shifting conversion for building-integrated photovoltaics. This comprehensive dataset is suitable for data driven analysis and models that may predict the efficiency of new LSCs without extensive experimental measurements. It can be continuously expanded and augmented in the future, offering the opportunity for data mining and may serve as training data for ML models.

Code availability

We hereby declare that no custom code was employed in the production or analysis of the data presented in this work.

References

1. Weber, W. H. & Lambe, J. Luminescent greenhouse collector for solar radiation. *Appl. Optics* **15**, 2299–2300 (1976).
2. Reisfeld, R. & Neuman, S. Planar solar-energy converter and concentrator based on uranyl-doped glass. *Nature* **274**, 144–145 (1978).
3. Meinardi, F., Bruni, F. & Brovelli, S. Luminescent solar concentrators for building-integrated photovoltaics. *Nat. Rev. Mater.* **2**, 17072 (2017).
4. Directive 2018/844 of the European Parliament and of the Council of 30 May 2018 amending Directive 2010/31/EU on the energy performance of buildings and Directive 2012/27/EU on energy efficiency. (Brussels, Belgium, 2018).
5. *Energy performance of buildings directive* https://energy.ec.europa.eu/topics/energy-efficiency/energy-efficient-buildings/energy-performance-buildings-directive_en (2010).
6. *Energy efficiency directive* https://energy.ec.europa.eu/topics/energy-efficiency/energy-efficiency-targets-directive-and-rules/energy-efficiency-directive_en (2012).
7. Kanellis, M., de Jong, M. M., Slooff, L. & Debije, M. G. The solar noise barrier project: 1. Effect of incident light orientation on the performance of a large-scale luminescent solar concentrator noise barrier. *Renew. Energy* **103**, 647–652 (2017).
8. Debije, M. G., Tzikas, C., Rajkumar, V. A. & de Jong, M. M. The solar noise barrier project: 2. The effect of street art on performance of a large scale luminescent solar concentrator prototype. *Renew. Energy* **113**, 1288–1292 (2017).
9. Debije, M. G., Tzikas, C., de Jong, M. M., Kanellis, M. & Slooff, L. H. The solar noise barrier project: 3. The effects of seasonal spectral variation, cloud cover and heat distribution on the performance of full-scale luminescent solar concentrator panels. *Renew. Energy* **116**, 335–343 (2018).
10. Bognar, A. *et al.* The solar noise barrier project 4: Modeling of full-scale luminescent solar concentrator noise barrier panels. *Renew. Energy* **151**, 1141–1149 (2020).
11. Keil, J., Liu, Y. L., Kortshagen, U. & Ferry, V. E. Bilayer luminescent solar concentrators with enhanced absorption and efficiency for agrivoltaic applications. *ACS Appl. Energy Mater.* **4**, 14102–14110 (2021).
12. Essahili, O., Ouafi, M. & Moudam, O. Recent progress in organic luminescent solar concentrators for agrivoltaics: opportunities for rare-earth complexes. *Sol. Energy* **245**, 58–66 (2022).
13. *Glass to Power SpA* https://www.glasstopower.com/ (2023).
14. *UbiQD - Ubiquitous Quantum Dots* https://ubiqd.com/ (2022).
15. *ClearVue - Energy Efficient, Energy Generating, Clear Glass* https://www.clearvuepv.com/ (2021).

16. Correia, S. F. H. *et al*. Autonomous power temperature sensor based on window-integrated transparent PV using sustainable luminescent carbon dots. *Nanoscale Adv.* **5**, 3428–3438 (2023).
17. Correia, S. F. H. *et al*. Bio-based solar energy harvesting for onsite mobile optical temperature sensing in smart cities. *Adv. Sci.* **9**, 2104801 (2022).
18. Meinardi, F. *et al*. Large-area luminescent solar concentrators based on 'Stokes-shift-engineered' nanocrystals in a mass-polymerized PMMA matrix. *Nat. Photonics* **8**, 392–399 (2014).
19. Ferreira, R. A. S., Correia, S. F. H., Monguzzi, A., Liu, X. & Meinardi, F. Spectral converters for photovoltaics – what's ahead. *Mater. Today* **33**, 105–121 (2020).
20. Zhang, B. L. *et al*. High-performance large-area luminescence solar concentrator incorporating a donor-emitter fluorophore system. *ACS Energy Lett.* **4**, 1839–1844 (2019).
21. Mateen, F. *et al*. Large-area luminescent solar concentrator utilizing donor-acceptor luminophore with nearly zero reabsorption: Indoor/outdoor performance evaluation. *J. Lumin.* **231**, 117837 (2021).
22. Meinardi, F. *et al*. Highly efficient large-area colourless luminescent solar concentrators using heavy-metal-free colloidal quantum dots. *Nat. Nanotechnol.* **10**, 878–885 (2015).
23. Brennan, L. J. *et al*. Large area quantum dot luminescent solar concentrators for use with dye-sensitised solar cells. *J. Mater. Chem. A* **6**, 2671–2680 (2018).
24. Meinardi, F. *et al*. Highly efficient luminescent solar concentrators based on earth-abundant indirect-bandgap silicon quantum dots. *Nat. Photonics* **11**, 177–185 (2017).
25. Li, H. B., Wu, K. F., Lim, J., Song, H. J. & Klimov, V. I. Doctor-blade deposition of quantum dots onto standard window glass for low-loss large-area luminescent solar concentrators. *Nat. Energy* **1**, 16157 (2016).
26. Wu, K. F., Li, H. B. & Klimov, V. I. Tandem luminescent solar concentrators based on engineered quantum dots. *Nat. Photonics* **12**, 105–110 (2018).
27. Li, X. Y. *et al*. Low-loss, high-transparency luminescent solar concentrators with a bioinspired self-cleaning surface. *J. Phys. Chem. Lett.* **13**, 9177–9185 (2022).
28. Corsini, F. *et al*. Large-area semi-transparent luminescent solar concentrators based on large Stokes shift aggregation-induced fluorinated emitters obtained through a sustainable synthetic approach. *Adv. Opt. Mater.* **9**, 2100182 (2021).
29. Aste, N., Tagliabue, L. C., Del Pero, C., Testa, D. & Fusco, R. Performance analysis of a large-area luminescent solar concentrator module. *Renew. Energy* **76**, 330–337 (2015).
30. Yang, C. C. *et al*. Impact of Stokes shift on the performance of near-infrared harvesting transparent luminescent solar concentrators. *Sci. Rep.* **8**, 16359 (2018).
31. Richards, B. S. & Howard, I. A. Luminescent solar concentrators for building integrated photovoltaics: opportunities and challenges. *Energy Environ. Sci.* **16**, 3214–3239 (2023).
32. Yang, C. H. *et al*. High-performance near-infrared harvesting transparent luminescent solar concentrators. *Adv. Opt. Mater.* **8**, 1901536 (2020).
33. Mazzaro, R. & Vomiero, A. The renaissance of luminescent solar concentrators: the role of inorganic nanomaterials. *Adv. Energy Mater.* **8**, 1801903 (2018).
34. de Bruin, T. A. & van Sark, W. G. J. H. M. Optimising absorption in luminescent solar concentrators constraint by average visible transmission and color rendering index. *Front. Phys.* **10**, 856799 (2022).
35. Maddox, J. Crystals from first principles. *Nature* **335**, 201 (1988).
36. Zhang, B. L., Lyu, G., Kelly, E. A. & Evans, R. C. Forster resonance energy transfer in luminescent solar concentrators. *Adv. Sci.* **9**, 2201160 (2022).
37. Griffini, G. Host matrix materials for luminescent solar concentrators: recent achievements and forthcoming challenges. *Front. Mater.* **6**, 29 (2019).
38. Rafiee, M., Chandra, S., Ahmed, H. & McCormack, S. J. An overview of various configurations of luminescent solar concentrators for photovoltaic applications. *Opt. Mater.* **91**, 212–227 (2019).
39. Li, Y., Zhang, X., Zhang, Y., Dong, R. & Luscombe, C. K. Review on the role of polymers in luminescent solar concentrators. *J. Polym. Sci. A* **57**, 201–215 (2018).
40. Moraitis, P., Schropp, R. E. I. & van Sark, W. Nanoparticles for luminescent solar concentrators - a review. *Opt. Mater.* **84**, 636–645 (2018).
41. Yang, C. C. & Lunt, R. R. Limits of visibly transparent luminescent solar concentrators. *Adv. Opt. Mater.* **5**, 1600851 (2017).
42. van Sark, W. G. J. H. M. *et al*. Luminescent solar concentrators - a review of recent results. *Opt. Express* **16**, 21773–21792 (2008).
43. Hermann, A. M. Luminescent solar concentrators - a review. *Sol. Energy* **29**, 323–329 (1982).
44. Purcell-Milton, F. & Gun'ko, Y. K. Quantum dots for luminescent solar concentrators. *J. Mater. Chem.* **22**, 16687 (2012).
45. Debije, M. G. & Verbunt, P. P. C. Thirty years of luminescent solar concentrator research: Solar energy for the built environment. *Adv. Energy Mater.* **2**, 12–35 (2012).
46. Papakonstantinou, I. & Tummeltshammer, C. Fundamental limits of concentration in luminescent solar concentrators revised: the effect of reabsorption and nonunity quantum yield. *Optica* **2**, 841–849 (2015).
47. Castelletto, S. & Boretti, A. Luminescence solar concentrators: a technology update. *Nano Energy* **109**, 108269 (2023).
48. Yang, C. C. *et al*. Consensus statement: standardized reporting of power-producing luminescent solar concentrator performance. *Joule* **6**, 8–15 (2022).
49. Warner, T., Ghiggino, K. P. & Rosengarten, G. A critical analysis of luminescent solar concentrator terminology and efficiency results. *Sol. Energy* **246**, 119–140 (2022).
50. Reisfeld, R., Shamrakov, D. & Jorgensen, C. Photostable solar concentrators based on fluorescent glass-films. *Sol. Energy Mater. Sol. C.* **33**, 417–427 (1994).
51. Buffa, M., Carturan, S., Debije, M. G., Quaranta, A. & Maggioni, G. Dye-doped polysiloxane rubbers for luminescent solar concentrator systems. *Sol. Energy Mater. Sol. C.* **103**, 114–118 (2012).
52. Wei, M. Y. *et al*. Ultrafast narrowband exciton routing within layered perovskite nanoplatelets enables low-loss luminescent solar concentrators. *Nat. Energy* **4**, 197–205 (2019).
53. Huang, C. S. *et al*. Nano-domains assisted energy transfer in amphiphilic polymer conetworks for wearable luminescent solar concentrators. *Nano Energy* **76**, 105039 (2020).
54. Singh, A. K. Light management using $CsPbBr_3$ colloidal quantum dots for luminescent solar concentrators. *Methods Appl. Fluores.* **8**, 045008 (2020).
55. Gu, G. W. *et al*. Re-absorption-free perovskite quantum dots for boosting the efficiency of luminescent solar concentrator. *J. Lumin.* **248**, 118963 (2022).
56. Li, Z. L. *et al*. Solvent-solute coordination engineering for efficient perovskite luminescent solar concentrators. *Joule* **4**, 631–643 (2020).
57. Gu, G. W. *et al*. Optical characterization and photo-electrical measurement of luminescent solar concentrators based on perovskite quantum dots integrated into the thiol-ene polymer. *Appl. Phys. Lett.* **119**, 011905 (2021).
58. Wu, J. J. *et al*. Efficient and stable thin-film luminescent solar concentrators enabled by near-infrared emission perovskite nanocrystals. *Angew. Chem. Int. Edit.* **59**, 7738–7742 (2020).

59. Nikolaidou, K. *et al.* Hybrid perovskite thin films as highly efficient luminescent solar concentrators. *Adv. Opt. Mater.* **4**, 2126–2132 (2016).

60. Wei, T. *et al.* Mn-doped multiple quantum well perovskites for efficient large-area luminescent solar concentrators. *ACS Appl. Mater. Interfaces* **14**, 44572–44580 (2022).

61. Oh, H., Kang, G. & Park, M. Polymer-mediated *in situ* growth of perovskite nanocrystals in electrospinning: design of composite nanofiber-based highly efficient luminescent solar concentrators. *ACS Appl. Energy Mater.* **5**, 15844–15855 (2022).

62. Gu, Y. Z. *et al.* Highly transparent, dual-color emission, heterophase $Cs_3Cu_2I_5/CsCu_2I_3$ nanolayer for transparent luminescent solar concentrators. *ACS Appl. Mater. Interfaces* **13**, 40798–40805 (2021).

63. Bhosale, S. S. *et al.* Mn-doped organic-inorganic perovskite nanocrystals for a flexible luminescent solar concentrator. *ACS Appl. Energy Mater.* **4**, 10565–10573 (2021).

64. Zhang, Y. D. *et al.* $CsPbBr_3$ nanocrystal-embedded glasses for luminescent solar concentrators. *Sol. Energy Mater. Sol. C.* **238**, 111619 (2022).

65. Zdrazil, L. *et al.* Transparent and low-loss luminescent solar concentrators based on self-trapped exciton emission in lead-free double perovskite nanocrystals. *ACS Appl. Energy Mater.* **4**, 6445–6453 (2021).

66. Liu, G. J., Zavelani-Rossi, M., Han, G. T., Zhao, H. G. & Vomiero, A. Red-emissive carbon quantum dots enable high efficiency luminescent solar concentrators. *J. Mater. Chem. A* **11**, 8950–8960 (2023).

67. Gordon, C. K. *et al.* Heterostructured nanotetrapod luminophores for reabsorption elimination within luminescent solar concentrators. *ACS Appl. Mater. Interfaces* **15**, 17914–17921 (2023).

68. Jing, Q., Meng, X. Y., Wang, C. & Zhao, H. G. Exciton dynamic in pyramidal InP/ZnSe quantum dots for luminescent solar concentrators. *ACS Appl. Nano. Mater.* **6**, 4449–4454 (2023).

69. de Bruin, T. A. *et al.* Analysis of the 1 year outdoor performance of quantum dot luminescent solar concentrators. *Sol. RRL* **7**, 2201121 (2023).

70. Li, S. H. *et al.* High-efficiency liquid luminescent solar concentrator based on $CsPbBr_3$ quantum dots. *Opt. Express* **30**, 45120–45129 (2022).

71. Ebrahimisadr, S., Olyaeefar, B. & Ahmadi-Kandjani, S. Dual-luminophore efficient luminescent solar concentrator fabricated by low-cost 3D printing. *Phys. Scripta* **98**, 015833 (2023).

72. Yu, K. L. *et al.* Integration of conjugated copolymers-based luminescent solar concentrators with excellent color rendering and organic photovoltaics for efficiently converting light to electricity. *Adv. Opt. Mater.* **11**, 2202283 (2023).

73. You, Y. M. *et al.* High-efficiency luminescent solar concentrators based on composition-tunable eco-friendly core/shell quantum dots. *Chem. Eng. J.* **452**, 139490 (2023).

74. Wang, J. *et al.* Controlled synthesis of long-wavelength multicolor-emitting carbon dots for highly efficient tandem luminescent solar concentrators. *ACS Appl. Energy Mater.* **3**, 12230–12237 (2020).

75. Song, Z. H. *et al.* The trade-off between optical efficiency and aesthetic properties of InP/ZnS quantum dots based luminescent solar concentrators. *J. Lumin.* **256**, 119622 (2023).

76. Gao, L. P. *et al.* Free radical-resistant carbon dots for bulky luminescent solar concentrators with high optical efficiency. *ACS Appl. Nano Mater.* **5**, 7850–7857 (2022).

77. Liu, X., Benetti, D. & Rosei, F. Semi-transparent luminescent solar concentrators based on plasmon-enhanced carbon dots. *J. Mater. Chem. A* **9**, 23345–23352 (2021).

78. Li, J. R., Zhao, H. G., Zhao, X. J. & Gong, X. Red and yellow emissive carbon dots integrated tandem luminescent solar concentrators with significantly improved efficiency. *Nanoscale* **13**, 9561–9569 (2021).

79. Wu, Y. H. *et al.* Highly emissive carbon dots/organosilicon composites for efficient and stable luminescent solar concentrators. *ACS Appl. Energy Mater.* **5**, 1781–1792 (2022).

80. Han, Y., Zhao, X. J., Vomiero, A., Gong, X. & Zhao, H. G. Red and green-emitting biocompatible carbon quantum dots for efficient tandem luminescent solar concentrators. *J. Mater. Chem. C* **9**, 12255–12262 (2021).

81. Cai, C. *et al.* Efficiently boosting the optical performances of laminated luminescent solar concentrators via combing blue-white light-emitting carbon dots and green/red emitting perovskite quantum dots. *Appl. Surf. Sci.* **609**, 155313 (2023).

82. Gong, X., Zheng, S. Y., Zhao, X. J. & Vomiero, A. Engineering high-emissive silicon-doped carbon nanodots towards efficient large-area luminescent solar concentrators. *Nano Energy* **101**, 107617 (2022).

83. Zhang, Y. *et al.* Highly efficient multifunctional frosted luminescent solar concentrators with zero-energy nightscape lighting. *J. Mater. Chem. A* **10**, 22145–22154 (2022).

84. Li, J. R., Zhao, H. G., Zhao, X. J. & Gong, X. Boosting efficiency of luminescent solar concentrators using ultra-bright carbon dots with large Stokes shift. *Nanoscale Horiz.* **8**, 83–94 (2023).

85. Gordon, C. K. *et al.* Performance evaluation of solid state luminescent solar concentrators based on InP/ZnS-Rhodamine 101 hybrid inorganic-organic luminophores. *J. Phys. Chem. C* **126**, 19803–19815 (2022).

86. Liu, B. X., Wang, L. H., Gong, X., Zhao, H. G. & Zhang, Y. M. Large scale synthesis of carbon dots for efficient luminescent solar concentrators. *J. Mater. Chem. C* **10**, 18154–18163 (2022).

87. Cao, X. D. *et al.* High-performance luminescent solar concentrators based on the core/shell CdSe/ZnS quantum dots composed into thiol-ene polymer. *J. Lumin.* **252**, 119368 (2022).

88. Vishwanathan, B. *et al.* A comparison of performance of flat and bent photovoltaic luminescent solar concentrators. *Sol. Energy* **112**, 120–127 (2015).

89. Xu, Z. J., Portnoi, M. & Papakonstantinou, I. Micro-cone arrays enhance outcoupling efficiency in horticulture luminescent solar concentrators. *Opt. Lett.* **48**, 183–186 (2023).

90. Zhao, H. G. *et al.* Gram-scale synthesis of carbon quantum dots with a large Stokes shift for the fabrication of eco-friendly and high-efficiency luminescent solar concentrators. *Energy Environ. Sci.* **14**, 396–406 (2021).

91. Zdrazil, L. *et al.* A carbon dot-based tandem luminescent solar concentrator. *Nanoscale* **12**, 6664–6672 (2020).

92. Zhao, H. G., Liu, G. J. & Han, G. T. High-performance laminated luminescent solar concentrators based on colloidal carbon quantum dots. *Nanoscale Adv.* **1**, 4888–4894 (2019).

93. Saeidi, S., Rezaei, B., Irannejad, N. & Ensafi, A. A. Efficiency improvement of luminescent solar concentrators using upconversion nitrogen-doped graphene quantum dots. *J. Power Sources* **476**, 228647 (2020).

94. Xin, W. *et al.* Construction of highly efficient carbon dots-based polymer photonic luminescent solar concentrators with sandwich structure. *Nanotechnology* **33**, 305601 (2022).

95. Xu, B. *et al.* Construction of laminated luminescent solar concentrator "smart" window based on thermoresponsive polymer and carbon quantum dots. *Crystals* **12**, 1612 (2022).

96. Carlos, C. P. A. *et al.* Environmentally friendly luminescent solar concentrators based on optically efficient and stable green fluorescent protein. *Green Chem.* **22**, 4943–4951 (2020).

97. Sadeghi, S. *et al.* Ecofriendly and efficient luminescent solar concentrators based on fluorescent proteins. *ACS Appl. Mater. Interfaces* **11**, 8710–8716 (2019).

98. Frias, A. R. *et al.* Sustainable liquid luminescent solar concentrators. *Adv. Sustain. Syst.* **3**, 1800134 (2019).

99. Mulder, C. L. *et al.* Luminescent solar concentrators employing phycobilisomes. *Adv. Mater.* **21**, 3181–3185 (2009).

100. Wu, J. *et al.* Solid-state photoluminescent silicone-carbon dots/dendrimer composites for highly efficient luminescent solar concentrators. *Chem. Eng. J.* **422**, 130158 (2021).

101. Tummeltshammer, C., Taylor, A., Kenyon, A. J. & Papakonstantinou, I. Flexible and fluorophore-doped luminescent solar concentrators based on polydimethylsiloxane. *Opt. Lett.* **41**, 713–716 (2016).
102. Lin, H. C., Xie, P., Liu, Y., Zhou, X. & Li, B. J. Tuning luminescence and reducing reabsorption of CdSe quantum disks for luminescent solar concentrators. *Nanotechnology* **26** (2015).
103. Li, C. *et al.* Large Stokes shift and high efficiency luminescent solar concentrator incorporated with CuInS$_2$/ZnS quantum dots. *Sci. Rep.-UK* **5**, 1–9 (2015).
104. Liu, C. *et al.* Luminescent solar concentrators fabricated by dispersing rare earth particles in PMMA waveguide. *Int. J. Photoenergy* **2014**, 290952 (2014).
105. Erickson, C. S. *et al.* Zero-reabsorption doped-nanocrystal luminescent solar concentrators. *ACS Nano* **8**, 3461–3467 (2014).
106. Coropceanu, I. & Bawendi, M. G. Core/shell quantum dot based luminescent solar concentrators with reduced reabsorption and enhanced efficiency. *Nano. Lett.* **14**, 4097–4101 (2014).
107. El-Bashir, S. M., Barakat, F. M. & AlSalhi, M. S. Double layered plasmonic thin-film luminescent solar concentrators based on polycarbonate supports. *Renew. Energy* **63**, 642–649 (2014).
108. Bomm, J. *et al.* Fabrication and full characterization of state-of-the-art quantum dot luminescent solar concentrators. *Sol. Energy Mater. Sol. C.* **95**, 2087–2094 (2011).
109. Gallagher, S. J., Norton, B. & Eames, P. C. Quantum dot solar concentrators: electrical conversion efficiencies and comparative concentrating factors of fabricated devices. *Sol. Energy* **81**, 813–821 (2007).
110. Correia, S. F. H. *et al.* Large-area tunable visible-to-near-infrared luminescent solar concentrators. *Adv. Sustainable Syst.* **2**, 1800002 (2018).
111. Frias, A. R. *et al.* Sustainable luminescent solar concentrators based on organic-inorganic hybrids modified with chlorophyll. *J. Mater. Chem. A* **6**, 8712–8723 (2018).
112. Rondão, R. *et al.* High-performance near-infrared luminescent solar concentrators. *ACS Appl. Mater. Interfaces* **9**, 12540–12546 (2017).
113. Kaniyoor, A., McKenna, B., Comby, S. & Evans, R. C. Design and response of high-efficiency, planar, doped luminescent solar concentrators using organic–inorganic di-Ureasil waveguides. *Adv. Opt. Mater.* **4**, 444–456 (2015).
114. Wilson, L. R. *et al.* Characterization and reduction of reabsorption losses in luminescent solar concentrators. *Appl. Optics* **49**, 1651–1661 (2010).
115. Wang, X. *et al.* Europium complex doped luminescent solar concentrators with extended absorption range from UV to visible region. *Sol. Energy* **85**, 2179–2184 (2011).
116. Wang, T. X. *et al.* Luminescent solar concentrator employing rare earth complex with zero self-absorption loss. *Sol. Energy* **85**, 2571–2579 (2011).
117. Correia, S. F. H. *et al.* Scale up the collection area of luminescent solar concentrators towards metre-length flexible waveguiding photovoltaics. *Prog. Photovolt.: Res. Appl.* **24**, 1178–1193 (2016).
118. Freitas, V. T. *et al.* Eu^{3+}-based bridged silsesquioxanes for transparent luminescent solar concentrators. *ACS Appl. Mater. Interfaces* **7**, 8770–8778 (2015).
119. Correia, S. F. H., Lima, P. P., André, P. S., Ferreira, R. A. S. & Carlos, L. D. High-efficiency luminescent solar concentrators for flexible waveguiding photovoltaics. *Sol. Energy Mater. Sol. C.* **138**, 51–57 (2015).
120. Nolasco, M. M. *et al.* Engineering highly efficient Eu(III)-based tri-ureasil hybrids toward luminescent solar concentrators. *J. Mater. Chem. A* **1**, 7339–7350 (2013).
121. Machida, K., Li, H., Ueda, D., Inoue, S. & Adachi, G. Preparation and application of lanthanide complex incorporated ormosil composite phosphor films. *J. Lumin.* **87-9**, 1257–1259 (2000).
122. Graffion, J. *et al.* Luminescent coatings from bipyridine-based bridged silsesquioxanes containing Eu^{3+} and Tb^{3+} salts. *J. Mater. Chem.* **22**, 13279–13285 (2012).
123. Graffion, J. *et al.* Modulating the photoluminescence of bridged silsesquioxanes incorporating Eu^{3+}-complexed n,n'-diureido-2,2'-bipyridine isomers: application for luminescent solar concentrators. *Chem. Mater.* **23**, 4773–4782 (2011).
124. Misra, V. & Mishra, H. Photoinduced proton transfer coupled with energy transfer: Mechanism of sensitized luminescence of terbium ion by salicylic acid doped in polymer. *J. Chem. Phys.* **128**, 244701 (2008).
125. Correia, S. F. H. *et al.* Luminescent solar concentrators: challenges for lanthanide-based organic-inorganic hybrid materials. *J. Mater. Chem. A* **2**, 5580–5596 (2014).
126. Grigoryev, I. S. *et al.* Efficient luminescent solar concentrators based on defectless organic glasses containing novel ytterbium cyanoporphyrazine complex. *Nanotechnologies in Russia* **7**, 492–498 (2012).
127. Frias, A. R. *et al.* Transparent luminescent solar concentrators using Ln^{3+}-based ionosilicas towards photovoltaic windows. *Energies* **12**, 451 (2019).
128. Tonezzer, M. *et al.* Luminescent solar concentrators employing new Eu(TTA)$_3$phen-containing parylene films. *Prog. Photovol.: Res. Appl.* **23**, 1037–1044 (2015).
129. Nam, S. K., Kim, K., Kang, J. H. & Moon, J. H. Dual-sensitized upconversion-assisted, triple-band absorbing luminescent solar concentrators. *Nanoscale* **12**, 17265–17271 (2020).
130. Slooff, L. H. *et al.* A luminescent solar concentrator with 7.1% power conversion efficiency. *Phys. Status Sol. - RRL* **2**, 257–259 (2008).
131. Li, Y. L., Olsen, J., Nunez-Ortega, K. & Dong, W. J. A structurally modified perylene dye for efficient luminescent solar concentrators. *Sol. Energy* **136**, 668–674 (2016).
132. Waldron, D. L., Preske, A., Zawodny, J. M., Krauss, T. D. & Gupta, M. C. PbSe quantum dot based luminescent solar concentrators. *Nanotechnology* **28**, 095205 (2017).
133. Huang, J. *et al.* Triplex glass laminates with silicon quantum dots for luminescent solar concentrators. *Sol. RRL* **4**, 2000195 (2020).
134. Gao, S. *et al.* Highly efficient luminescent solar concentrators based on benzoheterodiazole dyes with large Stokes shifts. *Chem.-Eur. J.* **26**, 11013–11023 (2020).
135. ten Kate, O. M., Kramer, K. W. & van der Kolk, E. Efficient luminescent solar concentrators based on self-absorption free, Tm^{2+} doped halides. *Sol. Energy Mater. Sol. C.* **140**, 115–120 (2015).
136. Huang, H. Y. *et al.* Engineering ligand-metal charge transfer states in cross-linked gold nanoclusters for greener luminescent solar concentrators with solid-state quantum yields exceeding 50% and low reabsorption losses. *J. Phys. Chem. C* **122**, 20019–20026 (2018).
137. Huang, H. Y. *et al.* Eco-friendly luminescent solar concentrators with low reabsorption losses and resistance to concentration quenching based on aqueous-solution-processed thiolate-gold nanoclusters. *Nanotechnology* **28**, 375702 (2017).
138. Chen, W. *et al.* Heavy metal free nanocrystals with near infrared emission applying in luminescent solar concentrator. *Sol. RRL* **1**, 1700041 (2017).
139. Zhu, M. B. *et al.* Deep-red emitting zinc and aluminium co-doped copper indium sulfide quantum dots for luminescent solar concentrators. *J. Colloid. Interface Sci.* **534**, 509–517 (2019).
140. Liu, H. C. *et al.* Scattering enhanced quantum dots based luminescent solar concentrators by silica microparticles. *Sol. Energy Mater. Sol. C.* **179**, 380–385 (2018).
141. Bergren, M. R. *et al.* High-performance CuInS$_2$ quantum dot laminated glass luminescent solar concentrators for windows. *ACS Energy Lett.* **3**, 520–525 (2018).

142. Zhou, Y. F. *et al*. Colloidal carbon dots based highly stable luminescent solar concentrators. *Nano Energy* **44**, 378–387 (2018).
143. Li, Y. X., Miao, P., Zhou, W., Gong, X. & Zhao, X. J. N-doped carbon-dots for luminescent solar concentrators. *J. Mater. Chem. A* **5**, 21452–21459 (2017).
144. Zhao, H. G. *et al*. Zero-dimensional perovskite nanocrystals for efficient luminescent solar concentrators. *Adv. Funct. Mater.* **29**, 1902262 (2019).
145. Tong, J. Y. *et al*. Fabrication of highly emissive and highly stable perovskite nanocrystal-polymer slabs for luminescent solar concentrators. *J. Mater. Chem. A* **7**, 4872–4880 (2019).
146. Huang, H. Y. *et al*. Eco-friendly, high-loading luminescent solar concentrators with concurrently enhanced optical density and quantum yields while without sacrificing edge-emission efficiency. *Sol. RRL* **3**, 1800347 (2019).
147. Zhao, H. G. *et al*. Efficient and stable tandem luminescent solar concentrators based on carbon dots and perovskite quantum dots. *Nano Energy* **50**, 756–765 (2018).
148. Ma, W. W. *et al*. Carbon dots and AIE molecules for highly efficient tandem luminescent solar concentrators. *Chem. Commun.* **55**, 7486–7489 (2019).
149. Liu, G. J., Zhao, H. G., Diao, F. Y., Ling, Z. B. & Wang, Y. Q. Stable tandem luminescent solar concentrators based on CdSe/CdS quantum dots and carbon dots. *J. Mater. Chem. C* **6**, 10059–10066 (2018).
150. Zhao, H. G. Refractive index dependent optical property of carbon dots integrated luminescent solar concentrators. *J. Lumin.* **211**, 150–156 (2019).
151. Wang, Z. J., Zhao, X. J., Guo, Z. Z., Miao, P. & Gong, X. Carbon dots based nanocomposite thin film for highly efficient luminescent solar concentrators. *Org. Electron.* **62**, 284–289 (2018).
152. Talite, M. J. *et al*. Visible-transparent luminescent solar concentrators based on carbon nanodots in the siloxane matrix with ultrahigh quantum yields and optical transparency at high-loading contents. *J. Phys. Chem. Lett.* **11**, 567–573 (2020).
153. Talite, M. J. *et al*. Greener luminescent solar concentrators with high loading contents based on *in situ* cross-linked carbon nanodots for enhancing solar energy harvesting and resisting concentration induced quenching. *ACS Appl. Mater. Interfaces* **10**, 34184–34192 (2018).
154. Mateen, F., Ali, M., Oh, H. & Hong, S. K. Nitrogen-doped carbon quantum dot based luminescent solar concentrator coupled with polymer dispersed liquid crystal device for smart management of solar spectrum. *Sol. Energy* **178**, 48–55 (2019).
155. Gong, X. *et al*. Fabrication of high-performance luminescent solar concentrators using N-doped carbon dots/PMMA mixed matrix slab. *Org. Electron.* **63**, 237–243 (2018).
156. Liu, G. J., Mazzaro, R., Wang, Y. Q., Zhao, H. G. & Vomiero, A. High efficiency sandwich structure luminescent solar concentrators based on colloidal quantum dots. *Nano Energy* **60**, 119–126 (2019).
157. Liu, X. *et al*. Eco-friendly quantum dots for liquid luminescent solar concentrators. *J. Mater. Chem. A* **8**, 1787–1798 (2020).
158. Hill, S. K. E. *et al*. Poly(methyl methacrylate) films with high concentrations of silicon quantum dots for visibly transparent luminescent solar concentrators. *ACS Appl. Mater. Interfaces* **12**, 4572–4578 (2020).
159. Connell, R., Keil, J., Peterson, C., Hillmyer, M. A. & Ferry, V. E. CdSe/CdS-poly(cyclohexylethylene) thin film luminescent solar concentrators. *APL Mater.* **7**, 101123 (2019).
160. Anand, A. *et al*. Evidence for the band-edge exciton of CuInS₂ nanocrystals enables record efficient large-area luminescent solar concentrators. *Adv. Funct. Mater.* **30**, 1906629 (2020).
161. Mateen, F., Lee, S. Y. & Hong, S. K. Luminescent solar concentrators based on thermally activated delayed fluorescence dyes. *J. Mater. Chem. A* **8**, 3708–3716 (2020).
162. Parola, I. *et al*. Characterization of double-doped polymer optical fibers as luminescent solar concentrators. *Polymers* **11**, 1187 (2019).
163. Mazzaro, R. *et al*. Hybrid silicon nanocrystals for color-neutral and transparent luminescent solar concentrators. *ACS Photonics* **6**, 2303–2311 (2019).
164. Sethi, A., Chandra, S., Ahmed, H. & McCormack, S. Broadband plasmonic coupling and enhanced power conversion efficiency in luminescent solar concentrator. *Sol. Energy Mater. Sol. C.* **203**, 110150 (2019).
165. Mateen, F., Oh, H., Kang, J., Lee, S. Y. & Hong, S. K. Improvement in the performance of luminescent solar concentrator using array of cylindrical optical fibers. *Renew. Energy* **138**, 691–696 (2019).
166. Ma, W. W. *et al*. Large Stokes-shift AIE fluorescent materials for high-performance luminescent solar concentrators. *Org. Electron.* **73**, 226–230 (2019).
167. Lyu, G. P. *et al*. Luminescent solar concentrators based on energy transfer from an aggregation-induced emitter conjugated polymer. *ACS Appl. Polym. Mater.* **1**, 3039–3047 (2019).
168. Jo, K., Hong, S. & Kim, H. J. Optical properties of EVA films including V570 for transparent luminescent solar concentrator. *Appl. Sci. Converg. Tec.* **29**, 14–18 (2020).
169. Albano, G. *et al*. Synthesis of new bis[1-(thiophenyl)propynones] as potential organic dyes for colorless luminescent solar concentrators (LSCs). *Dyes Pigm.* **174**, 108100 (2020).
170. Sholin, V., Olson, J. D. & Carter, S. A. Semiconducting polymers and quantum dots in luminescent solar concentrators for solar energy harvesting. *J. Appl. Phys.* **101**, 123114 (2007).
171. Shcherbatyuk, G. V., Inman, R. H., Wang, C., Winston, R. & Ghosh, S. Viability of using near infrared PbS quantum dots as active materials in luminescent solar concentrators. *Appl. Phys. Lett.* **96**, 191901 (2010).
172. Della Sala, P. *et al*. First demonstration of the use of very large Stokes shift cycloparaphenylenes as promising organic luminophores for transparent luminescent solar concentrators. *Chem. Commun.* **55**, 3160–3163 (2019).
173. Inman, R. H., Shcherbatyuk, G. V., Medvedko, D., Gopinathan, A. & Ghosh, S. Cylindrical luminescent solar concentrators with near-infrared quantum dots. *Opt. Express* **19**, 24308–24313 (2011).
174. Liu, Y. Q. *et al*. Stable metal-halide perovskites for luminescent solar concentrators of real-device integration. *Nano Energy* **85**, 105960 (2021).
175. Fisher, M. *et al*. Flexible luminescent solar concentrators utilizing bio-derived tandem fluorophores. 3333–3338 (2012).
176. Flores-Pacheco, A., Lopez-Delgado, R. & Alvarez-Ramos, M. E. Performance evaluation of CdTe QDs luminescent solar concentrators by analytic and simulation models. *IEEE Phot. Spec. Conf.*, 2637–2639 https://doi.org/10.1109/Pvsc43889.2021.9519121 (2021).
177. Makarov, N. S. *et al*. Minimizing scaling losses in high-performance quantum dot luminescent solar concentrators for large-area solar windows. *ACS Appl. Mater. Interfaces* **14**, 29679–29689 (2022).
178. Wang, J. Y. *et al*. Quantum dot-based luminescent solar concentrators fabricated through the ultrasonic spray-coating method. *ACS Appl. Mater. Interfaces* **14**, 41013–41021 (2022).
179. Neo, D. C. J., Goh, W. P., Lau, H. H., Shanmugam, J. & Chen, Y. F. CuInS₂ quantum dots with thick ZnSeₓS₁₋ₓ shells for a luminescent solar concentrator. *ACS Appl. Nano Mater.* **3**, 6489–6496 (2020).
180. Zhou, Y. *et al*. Near infrared, highly efficient luminescent solar concentrators. *Adv. Energy Mater.* **6**, 1501913 (2016).
181. Dhamo, L. *et al*. Efficient luminescent solar concentrators based on environmentally friendly Cd-free ternary AIS/ZnS quantum dots. *Adv. Opt. Mater.* **9**, 2100587 (2021).
182. Zhao, H. G. *et al*. Absorption enhancement in "giant" core/alloyed-shell quantum dots for luminescent solar concentrator. *Small* **12**, 5354–5365 (2016).

183. Tan, L. *et al*. Ultrasmall PbS quantum dots: a facile and greener synthetic route and their high performance in luminescent solar concentrators. *J. Mater. Chem. A* **5**, 10250–10260 (2017).
184. Sumner, R. *et al*. Analysis of optical losses in high-efficiency CuInS$_2$-based nanocrystal luminescent solar concentrators: balancing absorption versus scattering. *J. Phys. Chem. C* **121**, 3252–3260 (2017).
185. Liu, G. J. *et al*. Role of refractive index in highly efficient laminated luminescent solar concentrators. *Nano Energy* **70**, 104470 (2020).
186. Jalali, H. B. *et al*. Exciton recycling via InP quantum dot funnels for luminescent solar concentrators. *Nano Res.* **14**, 1488–1494 (2021).
187. Flores-Pacheco, A., Lopez-Delgado, R. & Alvarez-Ramos, M. E. Determination of power conversion efficiency of CdTe QDs luminescent solar concentrators by analytic model and COMSOL photogeneration model. *Optik* **248**, 168024 (2021).
188. Hyldahl, M. G., Bailey, S. T. & Wittmershaus, B. P. Photo-stability and performance of CdSe/ZnS quantum dots in luminescent solar concentrators. *Sol. Energy* **83**, 566–573 (2009).
189. Li, S. *et al*. Low reabsorption and stability enhanced luminescent solar concentrators based on silica encapsulated quantum rods. *Sol. Energy Mater. Sol. C.* **206**, 110321 (2020).
190. Han, S. S. *et al*. Visibly transparent solar windows based on colloidal silicon quantum dots and front-facing silicon photovoltaic cells. *ACS Appl. Mater. Interfaces* **12**, 43771–43777 (2020).
191. Huang, J. *et al*. Large-area transparent "quantum dot glass" for building-integrated photovoltaics. *ACS Photonics* **9**, 2499–2509 (2022).
192. Han, S. S. *et al*. Luminescence-guided and visibly transparent solar concentrators based on silicon quantum dots. *Opt. Express* **30**, 26896–26911 (2022).
193. Mateen, F. *et al*. Tandem structured luminescent solar concentrator based on inorganic carbon quantum dots and organic dyes. *Sol. Energy* **190**, 488–494 (2019).
194. Liu, F. *et al*. Anhydride-terminated solid-state carbon dots with bright orange emission induced by weak excitonic electronic coupling. *ACS Appl. Mater. Interfaces* **14**, 5762–5774 (2022).
195. Chen, J. C., Zhao, H. G., Li, Z. L., Zhao, X. J. & Gong, X. Highly efficient tandem luminescent solar concentrators based on eco-friendly copper iodide based hybrid nanoparticles and carbon dots. *Energy Environ. Sci.* **15**, 799–805 (2022).
196. Huang, H. Y. *et al*. Utilizing host-guest interaction enables the simultaneous enhancement of the quantum yield and Stokes shift in organosilane-functionalized, nitrogen-containing carbon dots for laminated luminescent solar concentrators. *Nanoscale* **12**, 23537–23545 (2020).
197. Tatsi, E. *et al*. Thermoresponsive host polymer matrix for self-healing luminescent solar concentrators. *ACS Appl. Energy Mater.* **3**, 1152–1160 (2020).
198. Geervliet, T. A., Gavrila, I., Iasilli, G., Picchioni, F. & Pucci, A. Luminescent solar concentrators based on renewable polyester matrices. *Chem.-Asian J.* **14**, 877–883 (2019).
199. Albano, G., Colli, T., Biver, T., Aronica, L. A. & Pucci, A. Photophysical properties of new p-phenylene- and benzodithiophene-based fluorophores for luminescent solar concentrators (LSCs). *Dyes Pigm.* **178**, 108368 (2020).
200. Rosadoni, E. *et al*. Y-shaped alkynylimidazoles as effective push-pull fluorescent dyes for luminescent solar concentrators (LSCs). *Dyes Pigm.* **201**, 110262 (2022).
201. Meti, P. *et al*. Luminescent solar concentrator based on large-Stokes shift tetraphenylpyrazine fluorophore combining aggregation-induced emission and intramolecular charge transfer features. *Dyes Pigm.* **202**, 110221 (2022).
202. Brzeczek-Szafran, A., Richards, C. J., Lopez, V. M., Wagner, P. & Nattestad, A. Aesthetically pleasing, visible light transmissive, luminescent solar concentrators using a BODIPY derivative. *Phys. Status Solidi A* **215**, 1800551 (2018).
203. Mateen, F. *et al*. Thin-film luminescent solar concentrator based on intramolecular charge transfer fluorophore and effect of polymer matrix on device efficiency. *Polymers* **13**, 3770 (2021).
204. Portnoi, M., Sol, C., Tummeltshammer, C. & Papakonstantinou, I. Impact of curvature on the optimal configuration of flexible luminescent solar concentrators. *Opt. Lett.* **42**, 2695–2698 (2017).
205. Moraitis, P. *et al*. Should anisotropic emission or reabsorption of nanoparticle luminophores be optimized for increasing luminescent solar concentrator efficiency? *Sol. RRL* **4**, 2000279 (2020).
206. Edelenbosch, O. Y., Fisher, M., Patrignani, L., van Sark, W. G. J. H. M. & Chatten, A. J. Luminescent solar concentrators with fiber geometry. *Opt. Express* **21**, A503 (2013).
207. van Sark, W. *et al*. The "Electric Mondrian" as a luminescent solar concentrator demonstrator case study. *Sol. RRL* **1**, 1600015 (2017).
208. Wilson, L. R., Klampaftis, E. & Richards, B. S. Enhancement of power output from a large-area luminescent solar concentrator with 4.8x concentration via solar cell current matching. *IEEE J. Photovolt.* **7**, 802–809 (2017).
209. Portnoi, M. *et al*. All-silicone-based distributed Bragg reflectors for efficient flexible luminescent solar concentrators. *Nano Energy* **70**, 104507 (2020).
210. Giebink, N. C., Wiederrecht, G. P. & Wasielewski, M. R. Resonance-shifting to circumvent reabsorption loss in luminescent solar concentrators. *Nat. Photonics* **5**, 695–702 (2011).
211. Kocher-Oberlehner, G., Bardosova, M., Pemble, M. & Richards, B. S. Planar photonic solar concentrators for building-integrated photovoltaics. *Sol. Energy Mater. Sol. C.* **104**, 53–57 (2012).
212. Zettl, M., Mayer, O., Klampaftis, E. & Richards, B. S. Investigation of host polymers for luminescent solar concentrators. *Energy Technol.* **5**, 1037–1044 (2017).
213. Wu, Y. H. *et al*. Bright and multicolor emissive carbon dots/organosilicon composite for highly efficient tandem luminescent solar concentrators. *Carbon* **207**, 77–85 (2023).
214. Cao, X. D. *et al*. High-efficiency plasmonic luminescent solar concentrators based on thiol-ene polymer. *J. Lumin.* **260**, 119889 (2023).
215. Bertozzi, A. F., Picchi, A. & Pucci, A. Waterborne acrylic resin containing Luminescent Eu pigments for luminescent solar concentrators. *Macromol. Chem. Phys.* **224**, 2200392 (2023).
216. Rajaramanan, T. *et al*. Eco-friendly Egyptian blue (CaCuSiO) dye for luminescent solar concentrator applications. *Mater. Adv.* **4**, 4344–4348 (2023).
217. Levitt, J. A. & Weber, W. H. Materials for luminescent greenhouse solar collectors. *Appl. Optics* **16**, 2684–2689 (1977).
218. Decardona, M. S., Carrascosa, M., Meseguer, F., Cusso, F. & Jaque, F. Outdoor evaluation of luminescent solar concentrator prototypes. *Appl. Optics* **24**, 2028–2032 (1985).
219. Batchelder, J. S., Zewail, A. H. & Cole, T. Luminescent Solar Concentrators .2. Experimental and Theoretical-Analysis of Their Possible Efficiencies. *Appl. Optics* **20**, 3733–3754 (1981).
220. Neuroth, N. & Haspel, R. Glasses for luminescent solar concentrators. *Sol. Energy Mater.* **16**, 235–242 (1987).
221. Reisfeld, R., Eyal, M., Chernyak, V. & Zusman, R. Luminescent solar concentrators based on thin-films of polymethylmethacrylate on a polymethylmethacrylate support. *Sol. Energy Mater.* **17**, 439–455 (1988).
222. Mahen, E. C. S. *et al*. Highly efficient sandwich design thin film luminescent solar concentrators based on blue and green emissive MAPbBr3 perovskites nanostructures. *Mater. Lett.* **337**, 134008 (2023).
223. Zhao, Y. M., Meek, G. A., Levine, B. G. & Lunt, R. R. Near-Infrared harvesting transparent luminescent solar concentrators. *Adv. Opt. Mater.* **2**, 606–611 (2014).

224. Zhi, H. Q. *et al*. Engineering the optical properties of eco-friendly CuGaS/ZnS and CuGaInS/ZnS core/shell quantum dots for high-performance tandem luminescent solar concentrators. *Sol. RRL*, 2300641 https://doi.org/10.1002/solr.202300641 (2023).

225. Li, J. R., Chen, J. C., Zhao, X. J., Vomiero, A. & Gong, X. High-loading of organosilane-grafted carbon dots in high-performance luminescent solar concentrators with ultrahigh transparency. *Nano Energy* **115**, 108674 (2023).

226. Bartolini, M. *et al*. Orange/red benzo[1,2-b:4,5-b']dithiophene 1,1,5,5-tetraoxide-based emitters for luminescent solar concentrators: Effect of structures on fluorescence properties and device performances. *ACS Appl. Energ. Mater.* **6**, 4862–4880 (2023).

227. Arslan, A., Ozel, K., Atilgan, A. & Yildiz, A. Thin film luminescent solar concentrators fabricated for indoor applications. *Physica B* **661**, 414939 (2023).

228. Zang, J. H. *et al*. Carbon nanodot with highly localized excitonic emission for efficient luminescent solar concentrator. *Nanophotonics* **12**, 4117–4126 (2023).

229. Arrigo, A. *et al*. From waste to energy: luminescent solar concentrators based on carbon dots derived from surgical facemasks. *Mater. Adv.* **4**, 5200–5205 (2023).

230. Son, J. *et al*. A mechanoresponsive smart window based on multifunctional luminescent solar concentrator. *Sol. RRL* **7**, 2300445 (2023).

231. Xia, P. F. *et al*. Luminescent solar concentrators with dual functions of photovoltaic and piezoelectric properties for wireless self-powered speed measurement. *Adv. Energy. Mater.* **13**, 2301332 (2023).

232. Ramalho, J. F. C. B., Carneiro Neto, A. N., Carlos, L. D., André, P. S. & Ferreira, R. A. S. in *Handbook on the Physics and Chemistry of Rare Earths* Vol. 61 (eds Bünzli, J.-C. & Pecharsky, V. K.) Ch. 324, 31–128 (Elsevier Science, B. V., 2022).

233. Ramalho, J. F. C. B., Carlos, L. D., André, P. S. & Ferreira, R. A. S. mOptical sensing for the internet of things: a smartphone-controlled platform for temperature monitoring. *Adv. Photonics Res.* **6**, 2000211 (2021).

234. van Eck, N. J. & Waltman, L. Citation-based clustering of publications using CitNetExplorer and VOSviewer. *Scientometrics* **111**, 1053–1070 (2017).

235. van Eck, N. J. & Waltman, L. CitNetExplorer: A new software tool for analyzing and visualizing citation networks. *J. Informetr.* **8**, 802–823 (2014).

236. Kim, K., Nam, S. K., Cho, J. & Moon, J. H. Photon upconversion-assisted dual-band luminescence solar concentrators coupled with perovskite solar cells for highly efficient semi-transparent photovoltaic systems. *Nanoscale Adv.* **12**, 12426–12431 (2020).

237. Ha, S. J. *et al*. Upconversion-assisted dual-band luminescent solar concentrator coupled for high power conversion efficiency photovoltaic systems. *ACS Photonics* **5**, 3621–3627 (2018).

238. Cai, T. *et al*. Mn^{2+}/Yb^{3+} codoped $CsPbCl_3$ perovskite nanocrystals with triple-wavelength emission for luminescent solar concentrators. *Adv. Sci.* **7**, 2001317 (2020).

239. Bai, X. *et al*. Efficient and tuneable photoluminescent boehmite hybrid nanoplates lacking metal activator centres for single-phase white LEDs. *Nat. Commun.* **5**, 5702 (2014).

240. Dienel, T., Bauer, C., Dolamic, I. & Bruhwiler, D. Spectral-based analysis of thin film luminescent solar concentrators. *Sol. Energy* **84**, 1366–1369 (2010).

241. Krumer, Z., van Sark, W. G. J. H. M., Schropp, R. E. I. & Donega, C. D. Compensation of self-absorption losses in luminescent solar concentrators by increasing luminophore concentration. *Sol. Energy Mater. Sol. C.* **167**, 133–139 (2017).

242. Ferreira, R. A. S. *et al*. A comprehensive dataset of photonic features on spectral converters in energy harvesting and conversion applications, *figshare*, https://doi.org/10.6084/m9.figshare.24903387 (2023).

Acknowledgements

Author contributions

R.A.S. Ferreira and P.S. André contributed to research plan determination, acquisition of all data, data analysis, result discussion, and manuscript writing. S.F.H. Correia and L. Fu contributed to data acquisition, data analysis and manuscript writing. M. Antunes and P. Georgieva contributed to data analysis.

Competing interests

The authors declare no competing interests.

Additional information

Correspondence and requests for materials should be addressed to R.A.S.F. or P.S.A.

Reprints and permissions information is available at www.nature.com/reprints.

Publisher's note Springer Nature remains neutral with regard to jurisdictional claims in published maps and institutional affiliations.